Scalable Multi-Agent Reinforcement Learning through Intelligent Information Aggregation

Siddharth Nayak [1], **Kenneth Choi** [1], **Wenqi Ding** [1],
Sydney Dolan [1], **Karthik Gopalakrishnan** [2], **Hamsa Balakrishnan** [1]
[1] Massachusetts Institute of Technology
[2] Stanford University
{sidnayak, kenchoi, wenqi22, sydneyd, hamsa}@mit.edu
kgopalakrishnan@stanford.edu

Abstract

We consider the problem of multi-agent navigation and collision avoidance when observations are limited to the local neighborhood of each agent. We propose InforMARL, a novel architecture for multi-agent reinforcement learning (MARL) which uses local information intelligently to compute paths for all the agents in a decentralized manner. Specifically, InforMARL aggregates information about the local neighborhood of agents for both the actor and the critic using a graph neural network and can be used in conjunction with any standard MARL algorithm. We show that (1) in training, InforMARL has better sample efficiency and performance than baseline approaches, despite using less information, and (2) in testing, it scales well to environments with arbitrary numbers of agents and obstacles.

1 Introduction

Reinforcement Learning (RL) has seen wide-ranging successes recently in high-dimensional robot control [1, 2], solving physics-based control problems [3], playing Go [4], Chess [5] and Atari video games [6, 7], etc. However, challenges remain in many real-world applications in which the tasks cannot be handled by a single agent, e.g., multi-player games, search-and-rescue drone missions, etc. [8]. In such cases, multiple agents may need to work together and share information in order to accomplish the task [9]. Naïve extensions of single-agent RL algorithms to multi-agent settings do not work well because of the non-stationarity in the environment, i.e. the actions of one agent affect the actions of others [10, 11]. Furthermore, tasks may require cooperation among the agents. Classical approaches to optimal planning may (1) be computationally intractable, especially for real-time applications, and (2) be unable to account for complex interactions and shared objectives between multiple agents. The ability of RL to learn by trial-and-error makes it well-suited for problems in which optimization-based methods are not effective. In particular, multi-agent reinforcement learning (MARL) approaches may be suitable in these situations due to their fast run-times and superior performance, and their ability to model shared goals between agents using appropriate reward structures.

In this paper, we focus on the multi-agent navigation and collision avoidance problem, where there are N agents navigating to their respective goals in a 2D environment with static and/or dynamic obstacles. The agents are assumed to be collaborative, i.e. the rewards are shared across all agents. We assume that an agent can only sense the presence of obstacles or other agents within a certain limited radius r. The overarching objective is for all the agents to reach their goals in the shortest time possible, while avoiding collisions with other agents and obstacles. This problem setting is quite general and arises in many contexts, *e.g.*, search-and-rescue robot teams [12], environmental monitoring [13], and drone delivery systems [14, 15, 16].

Preprint. Under review.

MARL-based techniques have achieved significant successes in recent times, *e.g.*, DeepMind's AlphaStar surpassing professional level players in StarCraft II [17], OpenAI Five defeating the world-champion in Dota II [18], etc. The performance of many of these MARL algorithms depends on the amount of information included in the state given as input to the neural networks [19]. In many practical multi-agent scenarios, each agent aims to share as little information as possible to accomplish the task at hand. This structure naturally arises in many multi-agent navigation settings, where agents may have a desired end goal but do not want to share their information due to communication constraints or proprietary concerns [20, 21]. These scenarios result in a decentralized structure, as agents only have locally available information about the overall system's state. In this paper, we focus on the question: "*Can we train scalable multi-agent reinforcement learning policies that use limited local information about the environment to perform collision-free navigation effectively?*"

We propose *InforMARL*, an approach for solving the multi-agent navigation problem using graph-reinforcement learning. The main features of our approach are that it: (1) uses a graph representation of the navigation environment which enables local information-sharing across the edges of the graph; (2) transfers well to different numbers of agents; and (3) achieves better sample complexity in training compared to prior approaches by aggregating relevant local information from neighbors in the underlying graph.

More broadly, our work (1) demonstrates that graphs provide a valuable abstraction for multi-agent navigation environments; (2) highlights that more information (i.e., global information as states) may not necessarily improve performance, and can, in fact, overwhelm the RL agent networks and lead to increased sample complexity; and (3) shows how graph architectures can identify the most valuable information for navigation from local observations to improve performance and scalability.

The rest of this paper is organized as follows. In Section 2, we briefly summarize recent developments in MARL under different settings. In Section 3, we describe InforMARL, our method for multi-agent navigation in settings with limited observability and communication. In Section 4, we show the effectiveness of InforMARL in learning policies for navigation by comparing its performance to other baseline algorithms. We also perform experiments on transferring InforMARL to scenarios with a different number of entities in the environment. Finally, in Section 5, we discuss the main conclusions of this paper and describe promising directions for future work.

2 Related Work

In this section, we discuss prior approaches to scaling MARL algorithms, as well as some recent work on information-sharing between agents in multi-agent systems.

2.1 Scaling MARL

Research on scaling MARL algorithms has broadly followed two main themes: (1) decentralized execution, and (2) transferring learning between scenarios.

Decentralized MARL: A popular approach to improve scaling is the centralized-training-decentralized-execution (CTDE) framework. Typically, CTDE frameworks utilize actor-critic methods [22], where the training step uses a centralized critic that incorporates global information from all actors. However, during execution, the agents use their own actor networks to select their actions in a decentralized manner to improve scalability. MADDPG [23] builds upon DDPG [1] by learning a centralized critic that is provided the joint state and actions of all agents. MATD3 [24] uses a double-centralized critic model, which helps reduce the over-estimation bias. In [19], the authors show the effectiveness of PPO in several standard multi-agent environments. In value-based methods, VDN [25] decomposes a centralized value function to a sum of individual agent-specific functions. Q-Mix [26] improves upon this by imposing a monotonicity requirement on agents' individual value functions and using a learnable mixing of the individual functions instead of only summing them as done in VDN. These MARL algorithms perform well in the navigation environment when they have access to information about the positions of all entities in the environment. But, as we demonstrate in this work, they fail to learn when that information is restricted to just local neighborhoods around the agents.

Transferability in MARL: It is desirable to have MARL formulations where the number of agents/entities in the environment doesn't hinder the performance of the model. Most of the previous

works using MARL for the navigation task require concatenation of observations of other entities in the environment to be able to learn meaningful policies. As the neural network size depends on the state input dimensions used while training, the learned policy fails to work in scenarios with a different number of entities in the environment. With the recent success of graph neural networks, many recent works have focused on leveraging the inherent graph structure present in multi-agent problems and tackling the issue of transferability. Zhou et al. [27] create a neighborhood graph according to how close the entities are to each other and use imitation learning to imitate a greedy behavior for the target-coverage problem [28, 29]. Similarly, Khan et al. [30] use graph neural networks with vanilla policy gradient [31] for the formation flying task [32, 33]. They show that dynamic graphs have worse performance than static graphs due to the large number of possible graphs the model has to learn. At the beginning of each episode, their model determines the connectivity of the agents with each other and uses the same graph over the whole episode. This works well for the formation flying task as the graph structure does not change much if the agents fly in the same formation over an episode.

DGN [34] combines a graph convolutional neural network [35] architecture with multi-head attention [36] for a variety of multi-agent environments, including 2D coverage and tracking. The DGN architecture assumes that each agent communicates with its three closest neighbors. Communicating with the three closest agents leads to a graph that is always connected. However, the three-agent connectivity assumption is highly restrictive in real life applications, as communication is generally restricted by mutual separation due to hardware constraints.

We use a distance-based agent-entity graph similar to Entity-Message Passing (EMP) [37]. However, the EMP architecture assumes that the agents have access to the positions of all entities in the environment at the beginning of the episode, which is not possible in the navigation setting where there are occluded static or dynamic obstacles. By contrast, our model does not require information on the positions of all entities at the beginning of the episode.

2.2 Information Sharing for MARL

For various cooperative tasks where explicit coordination is required to solve the task, enabling communication to share information across the agents helps with the performance. In CommNet [38], the authors introduce a model to learn a differentiable communication protocol between multiple agents. However, this communication does not explicitly model the interactions between the agents and rather used an averaged state of all the neighboring agents. VAIN [39] improves upon CommNet by using an exponential kernel-based attention to choose which specific messages from other agents to attend to. Similarly, ATOC [40] and TarMAC [41] use an attention mechanism for communication among agents but without any restrictions on which agent can communicate with which others, leading to a centralized setting during execution. GAXNET [42] also uses an attention mechanism [36], but additionally allows for the exchanging of attention weights with other agents to reduce the attention mismatch between them. While they show that their model works well for the navigation task, their formulation requires the maximum number of agents in the environment to be fixed before training. Our work also uses an attention mechanism for inter-agent communication. However, we do not have any message passing between objects in the environment (also referred to as 'entities') and agents; instead, the agents themselves do all the computation with local information of the entities' states.

3 Description of InforMARL

Our MARL framework for navigation, InforMARL, consists of four modules, as shown in Figure 1. We describe each in detail below.

3.1 Environment

Every object in the environment (also known as an 'entity') is assumed to be either an agent, an obstacle, or a goal. We define an agent-entity graph with respect to agent i at each time-step t, as $g_t^{(i)} \in \mathcal{G} : (\mathcal{V}, \mathcal{E})$, where each node $v \in \mathcal{V}$ is an entity in the environment. The variable $\texttt{entity\_type(j)} \in \{\texttt{agent}, \texttt{obstacle}, \texttt{goal}\}$ determines the type of entity at node j. There exists an edge $e \in \mathcal{E}$ between an agent and an entity if they are within a 'sensing radius' ρ of each other.

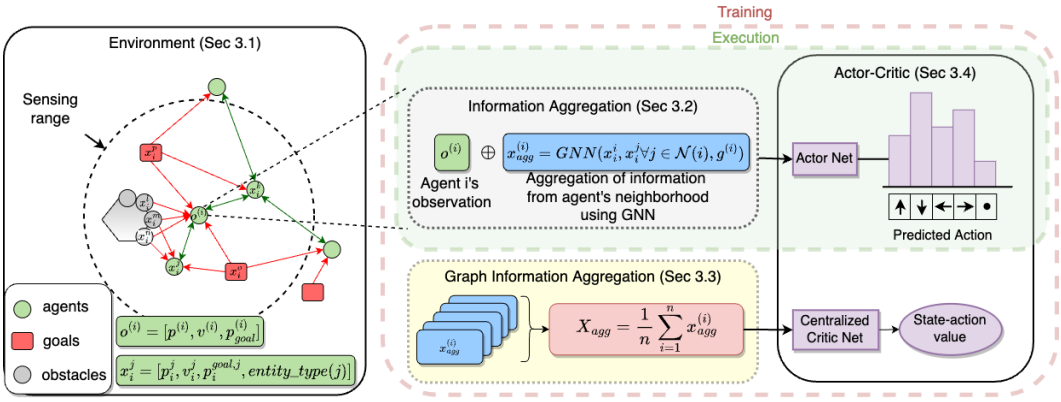

Figure 1: Overview of InforMARL. (i) Environment: The agents are depicted by green circles, the goals are depicted by red rectangles, and the unknown obstacles are depicted by gray circles. $x^{(i)}_{agg}$ represents the aggregated information from the neighborhood, which is the output of the GNN. A graph is created by connecting entities within the sensing-radius of the agents. (ii) Information Aggregation: Each agent's observation is concatenated with $x^{(i)}_{\text{agg}}$. The inter-agent edges are bidirectional, while the edges between agents and non-agent entities are unidirectional. (iii) Graph Information Aggregation: The aggregated vector from all the agents is averaged to get X_{agg}. (iv) Actor-Critic: The concatenated vector $[o^{(i)}, x^{(i)}_{\text{agg}}]$ is fed into the actor network to get the action, and X_{agg} is fed into the critic network to get the state-action values. The code for InforMARL is available at: https://github.com/nsidn98/InforMARL

The agent-agent edges are bidirectional, whereas the agent-non-agent edges are unidirectional (i.e. messages can only be passed from the non-agent entity to the agent). In other words, a unidirectional edge is equivalent to the agent sensing a nearby entity's state, while a bidirectional edge is equivalent to a communication channel between agents. This structure is similar to the agent-entity graph defined in [37], but without the assumption that all agents have access to the positions of all entities at the beginning of each episode. Note that our formulation also supports cases where disconnected sub-graphs are formed due to the positioning of the entities in the environment.

The corresponding Decentralized Partially Observable Markov Decision Process (Dec-POMDP) [43, 44, 45] is characterized by the tuple $\langle N, S, O, \mathcal{A}, \mathcal{G}, P, R, \gamma \rangle$, where N is the number of agents, $s \in S = \mathbb{R}^{N \times D}$ is the state space of the environment and D is the dimension of the state, and $o^{(i)} = O(s^{(i)}) \in \mathbb{R}^d$ is the local observation for agent i, where $d \leq D$ is the observation dimension. $a^{(i)} \in \mathcal{A}$ is the action space for agent i and the joint action for all N agents is given by $A = (a^{(1)}, \cdots, a^{(N)})$. Specifically, $a^{(i)}$ is a one-hot vector of size equal to the number of possible actions. $g^{(i)} \in \mathcal{G}(s; i)$ is the graph network formed by the entities in the environment with respect to agent i. $P(s'|s, A)$ is the transition probability from s to s' given the joint action A. $R(s, A)$ is the joint reward function. $\gamma \in [0, 1)$ is the discount factor. The MARL training process seeks to find an optimal policy, $\Pi = \left(\pi^{(1)}, \cdots, \pi^{(N)}\right)$, where each agent uses a policy $\pi^{(i)}_\theta \left(a^{(i)}|o^{(i)}, g^{(i)}\right)$ parameterized by θ to determine its action $a^{(i)}$ from its local observation $o^{(i)}$ and the graph network $g^{(i)}$ that it is a part of, while optimizing the discounted accumulated reward $J(\theta) = \mathbb{E}_{A_t, s_t}\left[\sum_t \gamma^t R\left(s_t, A_t\right)\right]$.

Agent i's local observation $o^{(i)}$ consists of its position and velocity in a global frame of reference and the relative position of the agent's goal with respect to its position. Each node j on the graph $g^{(i)}$ has node features $x_j = [p^j_i, v^j_i, p^{\text{goal},j}_i, \texttt{entity\_type(j)}]$ where $p^j_i, v^j_i, p^{\text{goal},j}_i$ are the *relative* position, velocity, and position of the goal of the entity at node j with respect to agent i, respectively. If node j corresponds to a (static/dynamic) obstacle or a goal, we set $p^{\text{goal},j}_i \equiv p^j_i$. Each edge e_{ij} has an associated edge feature given by the Euclidean distance between the entities i and j. For processing the `entity_type` categorical variable, we experimented with both using an embedding layer [46] and using one-hot encoding. No significant performance advantage with one method over the other was found, so we chose to use the embedding layer. Further analysis revealed that the learned embedding

vectors for `entity_type` were equidistant from each other when visualized in 2D. This was to be expected because each of the entity types $(agent, obstacle, goal)$ are equally distinct from another. Future work could include further refinement of `entity_type`, *e.g.*, adversarial vs. cooperative obstacles, static vs. dynamic obstacles, etc.

We adopt a similar reward function as used in multi-agent particle environment (MAPE)[1] [47] where each agent i gets a reward: $r_t^{(i)} = r_{\text{dist},t}^{(i)} + r_{\text{coll},t}^{(i)} + r_{\text{goal},t}^{(i)}$, where $r_{\text{dist},t}^{(i)}$ is the negative of the Euclidean distance to the goal, $r_{\text{coll},t}^{(i)} = -5$ if it collides with any other entity and zero otherwise, and $r_{\text{goal},t}^{(i)} = +5$ if the agent has reached the goal and zero otherwise. The joint reward function is defined as $R(s_t, A_t) = \sum_{i=1}^{N} r_t^{(i)}$, which encourages cooperation among all agents.

3.2 Information Aggregation

To infer information about the local neighborhood around each agent i, we use a graph neural network (GNN) with a message passing framework [48]. Specifically, we use Unified Message Passing Model (UniMP) [49], a variant of a graph transformer [36, 50] where each layer update is as follows:

$$x_i' = W_1 \cdot x_i + \sum_{j \in \mathcal{N}(i)} \alpha_{i,j} W_2 \cdot x_j, \tag{1}$$

where x_k are the node features in the graph, $\mathcal{N}(i)$ is the set of nodes which are connected to node i, W_k are learnable weight matrices and the attention coefficients $\alpha_{i,j}$ are computed via multi-head dot product attention:

$$\alpha_{i,j} = \text{softmax}\left(\frac{(W_3 \cdot x_i)^T (W_4 \cdot x_j + W_5 \cdot e_{ij})}{\sqrt{\text{c}}} \right), \tag{2}$$

where W_k are learnable weight matrices, e_{ij} are edge features for the edge connecting nodes i and j, and c is the output dimension for that specific layer.

The attention mechanism allows the agents to selectively prioritize messages coming from their neighbors according to their importance. We use multiple layers of this message-passing so that information can be propagated between agents that are higher-order neighbors with each other. For each agent i, this module aggregates information from the neighboring nodes in the graph into a fixed-sized vector $x_{\text{agg}}^{(i)}$. The concatenated vector $[o^{(i)}, x_{\text{agg}}^{(i)}]$ is given as the input to the actor network. This architecture allows InforMARL to dynamically adapt to a changing number of entities in the environment while remaining invariant to the permutation of the observed entities.

3.3 Graph Information Aggregation

While training the model in the CTDE setting, the critic generally gets the state-action pairs of all individual agents in the environment as a concatenated vector. To make the training transferable to a variable number of agents and to aid with curriculum learning [51, 52, 53], we replace this concatenation with a graph information aggregation module. This module is similar to the 'Information Aggregation' one in which a GNN aggregates information from the agent's neighbors. A global mean pooling operator is applied to aggregate the updated node features in the graph:

$$X_{\text{agg}} = \frac{1}{N} \sum_{i=1}^{N} x_{\text{agg}}^{(i)} \tag{3}$$

Note that X_{agg} is a vector of fixed size independent of the number of agents, which is not the case when concatenating the state action-pairs of all individual agents. This vector is then given as input to the critic network.

3.4 Actor-Critic Networks

The actor and critic networks can be either a multi-layer perceptron (MLP) or a recurrent neural network (RNN) [54], using either LSTMs [55] or GRUs [56]. Our proposed information aggregation

[1] https://github.com/openai/multiagent-particle-envs

method can be used in conjunction with any standard MARL algorithm (*e.g.*, MADDPG [23], MATD3 [24], MAPPO [19], QMIX [26], VDN [25], etc.).

4 Experiments

Task description: We evaluate our proposed model on the navigation task by modifying the MAPE [47]. In this environment, agents move around in a 2D space following a double integrator dynamics model [57]. The action space for each agent is discretized such that it can control unit acceleration and deceleration in the x- and y- directions. The navigation task differs from the target-coverage [28, 29] problem in that each agent navigates to its own specific goal rather than any of the available goals. Agents start at random locations at the beginning of each episode; the corresponding goals are also randomly distributed. Static obstacles are placed randomly in the environment in each episode. The overarching objective is for every agent to reach its corresponding goal without colliding with any other entity.

Implementation specifications: We chose to use MAPPO [19] as the base MARL algorithm for InforMARL because it was found to be the best performing of the standard MARL baselines in the 3 agent-3 obstacle scenario. We implemented InforMARL by modifying the official codebase for MAPPO [19] in PyTorch. The code for our experiments can be found at https://github.com/nsidn98/InforMARL. The codebase links to our baseline implementations can be found in Appendix A. We used the official implementations for most of the baselines considered in Section 4.2. We prefix the algorithm name with 'R' to denote the recurrent neural network (RNN) version of the algorithm (*e.g.* MAPPO-RMAPPO, MADDPG-RMADDPG, etc.). We use the same hyperparameters as used in the experiments for MAPPO, and do not perform parameter tuning on InforMARL for any of the MAPPO-based parameters. The hyperparameters used in our experiments can be found in Appendix B. We train the models with five different random seeds, and compute the means and standard deviations of the rewards.

Amount of information available to agents: The amount of information available to each agent determines whether or not the agent can learn a meaningful policy. Although having more information is generally correlated to better performance, it does not necessarily scale well with the number of agents. Prior works [19, 23] have typically used a naïve concatenation of the states of all agents or entities in the environment fed into a neural network. Such an approach scales poorly (the network input size is determined by the number of agents) and does not transfer well to scenarios with a different number of agents than the training environment. We illustrate the dependence of the learned policies on the amount of information available to agents by defining three information modes:

- *Local:* In the local information mode, $o^{(i)}_{\text{loc}} = [p^{(i)}, v^{(i)}, p^{(i)}_{\text{goal}}]$ where $p^{(i)}$ and $v^{(i)}$ are the position and velocity of agent i in a global frame, and $p^{(i)}_{\text{goal}}$ is the position of the goal relative to the agent's position. InforMARL uses this information mode.
- *Global:* Here, $o^{(i)}_{\text{glob}} = [p^{(i)}, v^{(i)}, p^{(i)}_{\text{goal}}, p^{(i)}_{\text{other}}]$, where $p^{(i)}_{\text{other}}$ comprises of the relative positions of all the other entities in the environment. The scenarios defined in the MAPE (and consequently, other approaches that use MAPE) use this type of information mode unless explicitly stated otherwise.
- *Neighborhood:* In this information mode, agent i observes $o^{(i)}_{\text{nbd}} = [p^{(i)}, v^{(i)}, p^{(i)}_{\text{goal}}, p^{(i)}_{\text{other}}]$, where $p^{(i)}_{\text{other}}$ comprises of the relative positions of all other entities which are within a distance `nbd-dist` of the agent. The maximum number of entities within the neighborhood is denoted `max-nbd-entities`, and so the dimension of the observation vector is fixed. If there are fewer than `max-nbd-entities` within a distance `nbd-dist` of the agent, we pad this vector with zeros.

4.1 A Motivating Experiment

Using *local* or *neighborhood* information modes is preferable, since they are transferable to scenarios with a different number of entities in the environment. By contrast, the *global* information mode is not transferable to other scenarios. Figure 2 shows the rewards obtained during training using the three information modes. We use RMAPPO as the base MARL algorithm for the 3 agent-3 obstacle

scenario. We chose RMAPPO because it was found to be the best-performing MARL algorithm in the global information mode.

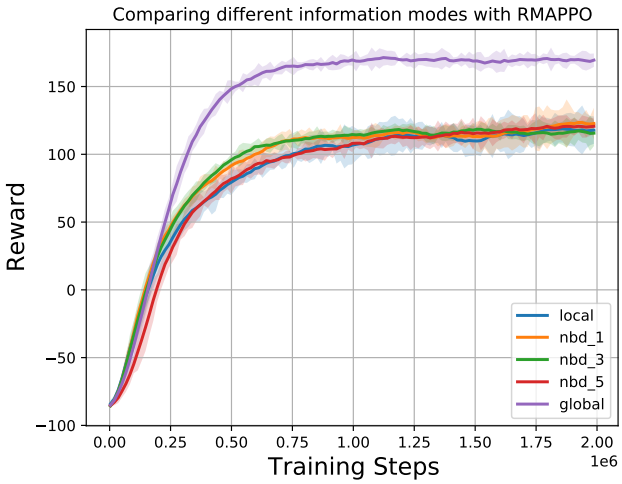

Figure 2: RMAPPO with the local, neighborhood (with 1, 3, and 5 `max-nbd-entities`), and global information given as states. The plots show the rewards during training for the 3 agent-3 obstacle navigation scenario. The means and standard deviations of the rewards over training with five random seeds are shown. Comparing the global information mode to the others, we see that merely providing local information and a naïve concatenation of neighborhood information is not sufficient to learn an optimal policy.

We see in Figure 2 that the policy learned with global information is better than the policies learned with local or neighborhood information. This is because it has the information necessary to take optimal actions. In the 'nbd_5' scenario, if all entities are within the `nbd_dist` ball, then $o^{(i)}_{\text{nbd}} \equiv o^{(i)}_{\text{glob}}$, since there are only five entities in the environment apart from the agent itself. Although the 'nbd_5' scenario is almost similar to the global information mode, the performances are not similar: the global information mode achieves much higher rewards. This behavior is because the observation $o_{i,\text{nbd}}$ can change temporally from having information about an entity when it lies within a `nbd_dist` ball of the agent, and then getting padded with zeros when it is out of the ball. This inconsistency in the amount of information accessible to the agent at every time step causes a significant performance difference between the policies learned with global and neighborhood information modes. This experiment motivates us to find a way in which more information can be leveraged (similar to the global case), but in a manner that does not suffer from the performance shortcomings of the neighborhood or local information modes.

4.2 Comparing InforMARL to Other Baselines

As shown in Section 4.1, using local information modes or naïvely concatenating neighborhood entity information is not sufficient to learn optimal policies. In this section, we demonstrate that InforMARL can effectively learn policies for navigation given local information. We then compare its performance in this problem setting with prior deep MARL approaches. Specifically, we consider the following classes of methods as baselines for comparison.

1. **Graph Policy Gradient (GPG) [30]:** GPG uses a graph convolutional neural network (GCN) [35] to parameterize policies for agents. The authors use the policy gradient method [31] as the base MARL algorithm. We perform experiments with both dynamic and static graphs. *Note: It was shown in [30] that using a static graph constructed at the beginning of the episode was better than using a dynamic graph.*
2. **Graph Convolutional Reinforcement Learning (DGN, DGN+ATOC) [40, 34]:** Similar to GPG, these methods use GCNs to capture interactions between the agents in the environment. A key difference between InforMARL and these two methods (GPG and DGN) is that while

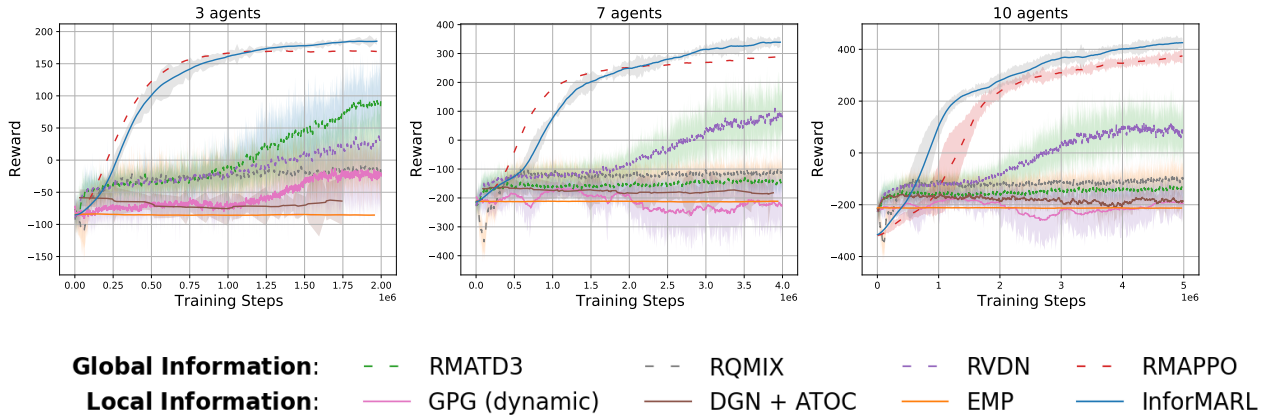

Figure 3: Comparison of the training performance of InforMARL with the best-performing baselines using global and local information. The means and standard deviations of the rewards over training with five random seeds are shown. InforMARL significantly outperforms most baseline algorithms. Although RMAPPO has similar performance, it requires global information. Appendix D presents a complete comparison to more baselines.

the latter two approaches consider only agents in their message-passing graph, InforMARL also includes other (non-agent) entities in the graph.

3. **Entity Message Passing (EMP) [37]:** Similar to InforMARL, EMP uses an agent-entity graph. However, in contrast to InforMARL, EMP assumes that agents know the positions of all entities in the graphs (i.e., global information) at the beginning of the episode.
4. **Other standard MARL Algorithms:** Finally, we compare InforMARL with standard MARL algorithms, namely, MADDPG [23], MATD3 [24], QMIX [26], VDN [25] and MAPPO [19]. In each case, we also consider the recurrent neural network versions. We focus on results for the global information modes, since our experiments found that these methods did not learn well with local information.

Figure 3 shows the training performance of InforMARL and the best-performing of the baselines mentioned above. For ease of visualization, we plot only the four best-performing methods with global and local information, respectively. A complete comparison plot showing all the baseline methods can be found in Appendix D. Each line corresponds to the mean and standard deviation over five random seeds. For each method, we consider scenarios with $N = 3$, $N = 7$, and $N = 10$ agents in the environment.

Figure 3 illustrates that only using RMAPPO (i.e. the RNN version of MAPPO) or InforMARL are agents able to learn to navigate and get to their goals. However, unlike RMAPPO which requires global information, InforMARL is able to achieve this with just local information. Furthermore, we find that InforMARL requires a similar number of training steps as RMAPPO, despite having access to much less information.

We present the following metrics in Table 1. The results represent an average over 100 test episodes.

1. The total rewards obtained by the agents during an episode using the reward function defined in Section 3.1. A higher value corresponds to better performance.
2. The fraction of an episode that the agents take on average to get to the goal, denoted T. If an agent does not reach its goal, then T is set to be 1 (lower is better).
3. Percent of episodes in which all agents are able to get to their goals, denoted $S\%$ (higher is better).
4. The total number of collisions (both agent-agent + agent-obstacle) that agents had in an episode, denoted # col. The lower this metric, the better the performance of the algorithm.

Although having a smaller number of collisions is better, the policies of some of the baseline algorithms do not significantly move the agents from their initial position after training and hence do

Algorithm	Information mode	$N = 3$				$N = 7$				$N = 10$			
		Reward	T	# col	$S\%$	Reward	T	# col	$S\%$	Reward	T	# col	$S\%$
MADDPG [23]	Global	-100.73	0.97	1.60	5	-206.07	0.98	6.01	0	-210.43	1.00	9.26	0
RMADDPG	Global	10.73	0.75	3.20	23	-122.069	0.95	9.75	3	-127.98	1.00	14.89	0
MATD3 [24]	Global	-90.31	0.98	1.11	5	-169.08	0.99	1.98	1	-173.20	1.00	3.50	0
RMATD3	Global	105.49	0.51	3.07	67	-128.93	0.96	7.40	6	-131.72	0.99	11.14	1
QMIX [26]	Global	-54.24	0.84	2.06	7	-288.81	0.97	17.05	0	-273.46	1.00	25.31	0
RQMIX	Global	19.21	0.77	1.42	28	-83.41	0.85	11.5	12	-76.98	0.96	17.04	2
VDN [25]	Global	18.86	0.67	2.29	27	39.87	0.64	8.58	23	43.23	0.73	12.54	19
RVDN	Global	64.04	0.62	1.05	45	140.94	0.62	6.60	47	157.63	0.64	10.00	43
RMAPPO [19]	**Global**	**173.13**	**0.41**	**1.47**	**96**	**327.39**	**0.44**	**8.64**	**88**	**366.81**	**0.44**	**13.21**	**79**
GPG (static) [30]	Local	-67.03	0.96	1.47	7	-180.14	0.99	6.41	1	-182.57	1.00	9.44	0
GPG (dynamic)	Local	-46.27	0.87	0.43	8	-165.91	1.00	3.20	3	-173.53	1.00	4.68	0
DGN [34]	Local	32.94	0.59	2.57	32	-232.32	0.97	5.39	0	-243.45	1.00	8.62	0
DGN + ATOC	Local	67.70	0.66	1.49	35	-189.61	0.97	2.20	0	-201.01	1.00	4.06	0
EMP [37]	Local	-83.96	0.98	1.35	6	-211.90	0.98	5.91	0	-209.90	1.00	9.22	0
InforMARL	**Local**	**205.24**	**0.38**	**1.45**	**100**	**399.01**	**0.37**	**6.97**	**100**	**429.14**	**0.39**	**10.50**	**100**

Table 1: Comparison of InforMARL with other baseline methods, for scenarios with 3, 7, and 10 agents in the environment. The results presented represent the average of 100 test episodes. The following metrics are compared: (a) Total reward obtained in an episode by all the agents (higher is better). (b) Fraction of episode taken by the agents to reach the goal, T (lower is better). (c) The total number of collisions the agents had in the episode, # col (lower is better). (d) Percent of episodes in which all agents are able to get to their goals, $S\%$ (higher is better). The best-performing methods that use global information (RMAPPO) and local information (InforMARL) are highlighted. As noted in Section 4.2, the metrics # col and S should be considered on balance.

not get to the goal. This leads to them having a lower number of collisions. Hence, this metric should be judged with the success rate in context.

The graph-based methods, namely GPG (static and dynamic), DGN (+ATOC), and EMP do not learn effectively with local information modes. Although both GPG and DGN use GCNs, they do not perform as well as InforMARL because they use only agent-agent and not agent-entity graphs. The lack of information about non-agent entities means that agents cannot maneuver through the environment to avoid collisions.

In contrast to the results showed in [30], our results show that the dynamic graph version of GPG is slightly better than the static graph one. A possible reason for this discrepancy is that the fixed formation environment considered in [30] is more amenable to the use of static graphs than the navigation environment. EMP, which uses a similar agent-entity graph as ours, fails to learn because of the strong assumption of having access to the positions of all entities in the environment at the beginning of the episode. The original implementation of EMP (and the associated environments) included information about all the entities other than agents in the observation vector.

4.3 Scalability of InforMARL

To evaluate the scalability of InforMARL with minimum information, we perform experiments by testing the models in scenarios with a different number of agents from those that they were trained on. Table 2 shows the results of testing InforMARL trained on n agents and tested on m agents. Each scenario is tested over 100 episodes. The number of obstacles in the environment is randomly chosen from $(0, 10)$ at the beginning of the episode. Based on the findings presented in Table 1) , we did not test the scalability of other methods since they did not perform well in the local information mode, or could not handle varying numbers of entities in the environment.

We see from Table 2 that InforMARL is able to achieve a success rate of 100% for almost all the scenarios. Furthermore, with InforMARL, the agents are able to get to their goals within $T \sim 0.39$ of the episode length in all scenarios. The number of collisions per agent increases, which is to

Test \ Train		$n = 3$	$n = 7$	$n = 10$
$m = 3$	Reward/m	68.41	58.30	57.27
	T	0.38	0.38	0.39
	(# col)/m	0.48	0.61	0.64
	$S\%$	100	100	99
$m = 7$	Reward/m	61.16	57.00	58.32
	T	0.38	0.37	0.38
	(# col)/m	1.15	0.99	1.03
	$S\%$	100	100	100
$m = 10$	Reward/m	58.59	53.25	52.10
	T	0.38	0.38	0.39
	(# col)/m	1.60	1.43	1.68
	$S\%$	100	99	100
$m = 15$	Reward/m	53.19	46.39	48.15
	T	0.39	0.39	0.40
	(# col)/m	2.24	2.314	2.20
	$S\%$	100	99	99

Table 2: Test performance of InforMARL, when trained on scenarios with n agents and tested on scenarios with m agents in the environment. InforMARL is able to achieve a success rate of nearly 100% while the fraction of episodes taken to reach the goals (T) is almost constant. Note that we normalize the reward and the number of collisions by m for ease of comparison.

be expected as the environment becomes denser. We believe that this can be remedied by using a stricter penalty (negative reward) for collisions instead of the -5 penalty used in our experiments. Alternatively, a more sophisticated approach with control barrier functions for satisfying safety constraints could be used to provide a formal safety guarantee in the MARL setting [58].

4.4 Effect of Sensing Radius

We investigate how the performance of InforMARL depends on the sensing radius, namely, how much information (i.e. over what neighborhood of the ego-agent) an agent has access to. As the radius increases to a large value, the graph becomes fully connected; as the radius decreases to zero, the neighborhood information mode converges to the local information mode. As seen in Figure 4, when learning with a small sensing radius (*e.g.* $\rho = \{0.1, 0.2\}$), the agents are not able to achieve the same reward as can be achieved with a larger sensing radius ($\rho = \{0.5, 1, 2, 5\}$)[2]. We also note that there are diminishing returns when increasing the sensing radius from $\rho = 0.5$ to $\rho = 5$. Since the agents far away from the ego-agent have little influence on its immediate decisions, the extra information obtained by increasing the sensing radius does not improve performance very much.

4.5 Ablation Study for Graph Information Aggregation Module

The graph information aggregation module allows our method to perform transfer learning to more complex environments. In this section, we compare models with and without the graph information aggregation module. In the absence of the graph information aggregation module, the states of individual agents are concatenated to be given as input to the centralized critic. Figure 5 presents the results of this ablation study. We find that both models have similar sample complexities and performance. However, the number of parameters for the critic network with the graph information aggregation module is much smaller and independent of the number of entities in the environment.

[2]Measurements for ρ, a distance, are in meters

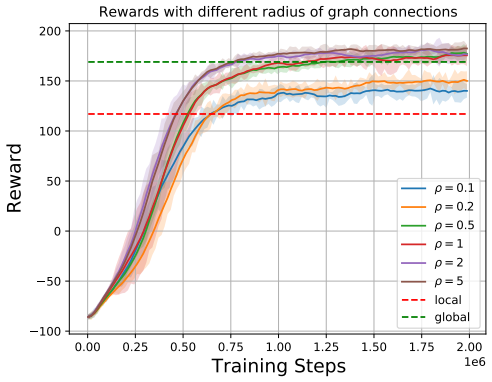

Figure 4: Diminishing returns in performance gains from increasing the sensing radius for InforMARL. The dashed lines are the reward values after saturation for RMAPPO in the global (in green) and local (in red) information modes, respectively. They are provided for reference.

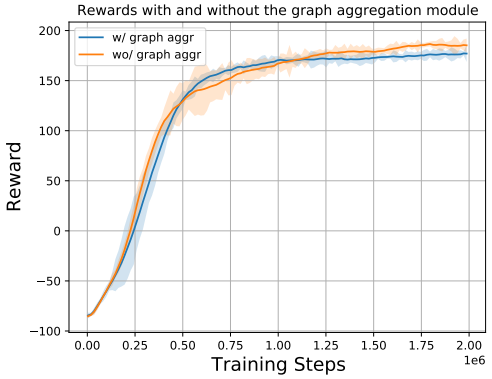

Figure 5: Training performance of InforMARL with, and without, the graph information aggregation module, for a 3-agent scenario. The two variants have similar sample complexities. However, the critic network with the graph information aggregation module has fewer parameters than the one without this module.

5 Conclusions and Future Work

We introduced InforMARL, a novel architecture that uses GNNs for scalable multi-agent reinforcement learning. We showed that having just local observations as states is not enough for standard MARL algorithms to learn meaningful policies. Along with this, we also showed that albeit naïvely concatenating state information about all the entities in the environment helps to learn good policies, they are not transferable to other scenarios with a different number of entities than what it was trained on. InforMARL is able to learn transferable policies using standard MARL algorithms using just local observations and an aggregated neighborhood information vector. Furthermore, it has better sample complexity than other standard MARL algorithms that use global observation. Future work will include the introduction of more complex (potentially adversarial) dynamic obstacles in the environment and adding a safety guarantee layer for the actions of the agents to avoid collisions. Additionally, the use of InforMARL for curriculum learning and transfer learning to different environments is a topic of ongoing research.

Acknowledgements

The authors would like to thank the MIT SuperCloud [59] and the Lincoln Laboratory Supercomputing Center for providing high performance computing resources that have contributed to the research results reported within this paper. The NASA University Leadership initiative (grant #80NSSC20M0163) provided funds to assist the authors with their research, but this article solely reflects the opinions and conclusions of its authors and not any NASA entity. This research was sponsored in part by the United States AFRL and the United States Air Force Artificial Intelligence Accelerator and was accomplished under Cooperative Agreement Number FA8750-19-2-1000. The views and conclusions contained in this document are those of the authors and should not be interpreted as representing the official policies, either expressed or implied, of the United States Air Force or the U.S. Government. The U.S. Government is authorized to reproduce and distribute reprints for Government purposes notwithstanding any copyright notion herein.

References

[1] Timothy P. Lillicrap, Jonathan J. Hunt, Alexander Pritzel, Nicolas Heess, Tom Erez, Yuval Tassa, David Silver, and Daan Wierstra. Continuous control with deep reinforcement learning. In Yoshua Bengio and Yann LeCun, editors, *4th International Conference on Learning Representations, ICLR 2016, San Juan, Puerto Rico, May 2-4, 2016, Conference Track Proceedings*, 2016.

[2] Sergey Levine, Chelsea Finn, Trevor Darrell, and Pieter Abbeel. End-to-end training of deep visuomotor policies. *CoRR*, abs/1504.00702, 2015.

[3] Nicolas Heess, Greg Wayne, David Silver, Timothy P. Lillicrap, Yuval Tassa, and Tom Erez. Learning continuous control policies by stochastic value gradients. *CoRR*, abs/1510.09142, 2015.

[4] David Silver, Aja Huang, Chris J. Maddison, Arthur Guez, Laurent Sifre, George van den Driessche, Julian Schrittwieser, Ioannis Antonoglou, Veda Panneershelvam, Marc Lanctot, and et al. Mastering the game of go with deep neural networks and tree search. *Nature*, 529(7587):484–489, 2016.

[5] David Silver, Thomas Hubert, Julian Schrittwieser, Ioannis Antonoglou, Matthew Lai, Arthur Guez, Marc Lanctot, Laurent Sifre, Dharshan Kumaran, Thore Graepel, Timothy P. Lillicrap, Karen Simonyan, and Demis Hassabis. Mastering chess and shogi by self-play with a general reinforcement learning algorithm. *CoRR*, abs/1712.01815, 2017.

[6] Volodymyr Mnih, Koray Kavukcuoglu, David Silver, Alex Graves, Ioannis Antonoglou, Daan Wierstra, and Martin A. Riedmiller. Playing atari with deep reinforcement learning. *CoRR*, abs/1312.5602, 2013.

[7] V. Mnih, K. Kavukcuoglu, D. Silver, Andrei A. Rusu, J. Veness, Marc G. Bellemare, A. Graves, Martin A. Riedmiller, A. Fidjeland, Georg Ostrovski, Stig Petersen, Charlie Beattie, A. Sadik, Ioannis Antonoglou, Helen King, D. Kumaran, Daan Wierstra, S. Legg, and D. Hassabis. Human-level control through deep reinforcement learning. *Nature*, 518:529–533, 2015.

[8] Sven Gronauer and Klaus Diepold. Multi-agent deep reinforcement learning: a survey. *Artificial Intelligence Review*, 55(2):895–943, 2022.

[9] Ming Tan. Multi-agent reinforcement learning: Independent vs. cooperative agents. In *Proceedings of the tenth international conference on machine learning*, pages 330–337, 1993.

[10] Ming Tan. Multi-agent reinforcement learning: Independent vs. cooperative agents. In *In Proceedings of the Tenth International Conference on Machine Learning*, pages 330–337. Morgan Kaufmann, 1993.

[11] Ardi Tampuu, Tambet Matiisen, Dorian Kodelja, Ilya Kuzovkin, Kristjan Korjus, Juhan Aru, Jaan Aru, and Raul Vicente. Multiagent cooperation and competition with deep reinforcement learning. *CoRR*, abs/1511.08779, 2015.

[12] Vijay Kumar, D. Rus, and Sanjiv Singh. Robot and sensor networks for first responders. *IEEE Pervasive Computing*, 3(4):24–33, 2004.

[13] Matthew Dunbabin and Lino Marques. Robots for environmental monitoring: Significant advancements and applications. *IEEE Robotics & Automation Magazine*, 19(1):24–39, 2012.

[14] Hanlin Zhang, Sixiao Wei, Wei Yu, Erik Blasch, Genshe Chen, Dan Shen, and Khanh Pham. Scheduling methods for unmanned aerial vehicle based delivery systems. In *2014 IEEE/AIAA 33rd Digital Avionics Systems Conference (DASC)*, pages 6C1–1–6C1–9, 2014.

[15] Kevin Dorling, Jordan Heinrichs, Geoffrey G. Messier, and Sebastian Magierowski. Vehicle routing problems for drone delivery. *IEEE Transactions on Systems, Man, and Cybernetics: Systems*, 47(1):70–85, 2017.

[16] Michelle Sing Yee Hii, Patrick Courtney, and Paul G. Royall. An evaluation of the delivery of medicines using drones. *Drones*, 3(3), 2019.

[17] Oriol Vinyals, Igor Babuschkin, Wojciech M. Czarnecki, Michaël Mathieu, Andrew Dudzik, Junyoung Chung, David H. Choi, Richard Powell, Timo Ewalds, Petko Georgiev, Junhyuk Oh, Dan Horgan, Manuel Kroiss, Ivo Danihelka, Aja Huang, L. Sifre, Trevor Cai, John P. Agapiou, Max Jaderberg, Alexander Sasha Vezhnevets, Rémi Leblond, Tobias Pohlen, Valentin Dalibard, David Budden, Yury Sulsky, James Molloy, Tom Le Paine, Caglar Gulcehre, Ziyun Wang, Tobias Pfaff, Yuhuai Wu, Roman Ring, Dani Yogatama, Dario Wünsch, Katrina McKinney, Oliver Smith, Tom Schaul, Timothy P. Lillicrap, Koray Kavukcuoglu, Demis Hassabis, Chris Apps, and David Silver. Grandmaster level in starcraft ii using multi-agent reinforcement learning. *Nature*, pages 1–5, 2019.

[18] Christopher Berner, Greg Brockman, Brooke Chan, Vicki Cheung, Przemyslaw Debiak, Christy Dennison, David Farhi, Quirin Fischer, Shariq Hashme, Christopher Hesse, Rafal Józefowicz, Scott Gray, Catherine Olsson, Jakub Pachocki, Michael Petrov, Henrique Pondé de Oliveira Pinto, Jonathan Raiman, Tim Salimans, Jeremy Schlatter, Jonas Schneider, Szymon Sidor, Ilya Sutskever, Jie Tang, Filip Wolski, and Susan Zhang. Dota 2 with large scale deep reinforcement learning. *CoRR*, abs/1912.06680, 2019.

[19] Chao Yu, Akash Velu, Eugene Vinitsky, Jiaxuan Gao, Yu Wang, Alexandre Bayen, and Yi Wu. The surprising effectiveness of PPO in cooperative multi-agent games. In *Thirty-sixth Conference on Neural Information Processing Systems Datasets and Benchmarks Track*, 2022.

[20] James Rendleman and Sarah Mountin. *Responsible SSA Cooperation to Mitigate On-orbit Space Debris Risks*, page 851–856. International Conference on Recent Advances in Space Technologies, 2015.

[21] Charity Weeden, Jonathan Goff, Jessica Noble, Jeremy Schiel, Dana Turse, Colin Doughan, John Carrico, and Rob Patterson. Comments of global newspace operators, 2019.

[22] Vijay Konda and John Tsitsiklis. Actor-critic algorithms. In S. Solla, T. Leen, and K. Müller, editors, *Advances in Neural Information Processing Systems*, volume 12. MIT Press, 1999.

[23] Ryan Lowe, Yi Wu, Aviv Tamar, Jean Harb, Pieter Abbeel, and Igor Mordatch. Multi-agent actor-critic for mixed cooperative-competitive environments. *CoRR*, abs/1706.02275, 2017.

[24] Johannes Ackermann, Volker Gabler, Takayuki Osa, and Masashi Sugiyama. Reducing overestimation bias in multi-agent domains using double centralized critics. *CoRR*, abs/1910.01465, 2019.

[25] Peter Sunehag, Guy Lever, Audrunas Gruslys, Wojciech Marian Czarnecki, Vinícius Flores Zambaldi, Max Jaderberg, Marc Lanctot, Nicolas Sonnerat, Joel Z. Leibo, Karl Tuyls, and Thore Graepel. Value-decomposition networks for cooperative multi-agent learning. *CoRR*, abs/1706.05296, 2017.

[26] Tabish Rashid, Mikayel Samvelyan, Christian Schröder de Witt, Gregory Farquhar, Jakob N. Foerster, and Shimon Whiteson. QMIX: monotonic value function factorisation for deep multi-agent reinforcement learning. *CoRR*, abs/1803.11485, 2018.

[27] Lifeng Zhou, Vishnu D. Sharma, Qingbiao Li, Amanda Prorok, Alejandro Ribeiro, and Vijay Kumar. Graph neural networks for decentralized multi-robot submodular action selection. *CoRR*, abs/2105.08601, 2021.

[28] Pratap Tokekar, Volkan Isler, and Antonio Franchi. Multi-target visual tracking with aerial robots. In *2014 IEEE/RSJ International Conference on Intelligent Robots and Systems*, pages 3067–3072, 2014.

[29] Philip Dames, Pratap Tokekar, and Vijay Kumar. Detecting, localizing, and tracking an unknown number of moving targets using a team of mobile robots. *The International Journal of Robotics Research*, 36(13-14):1540–1553, 2017.

[30] Arbaaz Khan, Ekaterina Tolstaya, Alejandro Ribeiro, and Vijay Kumar. Graph policy gradients for large scale robot control, 2019.

[31] Richard S Sutton, David McAllester, Satinder Singh, and Yishay Mansour. Policy gradient methods for reinforcement learning with function approximation. In S. Solla, T. Leen, and K. Müller, editors, *Advances in Neural Information Processing Systems*, volume 12. MIT Press, 1999.

[32] M. Turpin, Nathan Michael, and V. Kumar. Trajectory design and control for aggressive formation flight with quadrotors. *Autonomous Robots*, 33(1):143 – 156, August 2012.

[33] Matthew Turpin, Nathan Michael, and Vijay Kumar. Decentralized formation control with variable shapes for aerial robots. In *2012 IEEE International Conference on Robotics and Automation*, pages 23–30, 2012.

[34] Jiechuan Jiang, Chen Dun, Tiejun Huang, and Zongqing Lu. Graph convolutional reinforcement learning. In *ICLR*, 2020.

[35] Thomas N. Kipf and Max Welling. Semi-supervised classification with graph convolutional networks. *CoRR*, abs/1609.02907, 2016.

[36] Ashish Vaswani, Noam Shazeer, Niki Parmar, Jakob Uszkoreit, Llion Jones, Aidan N Gomez, Ł ukasz Kaiser, and Illia Polosukhin. Attention is all you need. In I. Guyon, U. Von Luxburg, S. Bengio, H. Wallach, R. Fergus, S. Vishwanathan, and R. Garnett, editors, *Advances in Neural Information Processing Systems*, volume 30. Curran Associates, Inc., 2017.

[37] Akshat Agarwal, Sumit Kumar, and Katia P. Sycara. Learning transferable cooperative behavior in multi-agent teams. *CoRR*, abs/1906.01202, 2019.

[38] Sainbayar Sukhbaatar, Arthur Szlam, and Rob Fergus. Learning multiagent communication with backpropagation. *CoRR*, abs/1605.07736, 2016.

[39] Yedid Hoshen. Vain: Attentional multi-agent predictive modeling. In I. Guyon, U. Von Luxburg, S. Bengio, H. Wallach, R. Fergus, S. Vishwanathan, and R. Garnett, editors, *Advances in Neural Information Processing Systems*, volume 30. Curran Associates, Inc., 2017.

[40] Jiechuan Jiang and Zongqing Lu. Learning attentional communication for multi-agent cooperation. *CoRR*, abs/1805.07733, 2018.

[41] Abhishek Das, Théophile Gervet, Joshua Romoff, Dhruv Batra, Devi Parikh, Michael G. Rabbat, and Joelle Pineau. Tarmac: Targeted multi-agent communication. *CoRR*, abs/1810.11187, 2018.

[42] Won Joon Yun, Byungju Lim, Soyi Jung, Young-Chai Ko, Jihong Park, Joongheon Kim, and Mehdi Bennis. Attention-based reinforcement learning for real-time UAV semantic communication. *CoRR*, abs/2105.10716, 2021.

[43] Martin L. Puterman. *Markov Decision Processes*. Wiley, 1994.

[44] Leslie Pack Kaelbling, Michael L. Littman, and Anthony R. Cassandra. Planning and acting in partially observable stochastic domains. *Artificial Intelligence*, 101(1):99–134, 1998.

[45] Frans A. Oliehoek and Christopher Amato. *A Concise Introduction to Decentralized POMDPs*. Springer Publishing Company, Incorporated, 1st edition, 2016.

[46] Tomás Mikolov, Ilya Sutskever, Kai Chen, Greg Corrado, and Jeffrey Dean. Distributed representations of words and phrases and their compositionality. *CoRR*, abs/1310.4546, 2013.

[47] Ryan Lowe, Yi Wu, Aviv Tamar, Jean Harb, Pieter Abbeel, and Igor Mordatch. Multi-agent actor-critic for mixed cooperative-competitive environments. *Neural Information Processing Systems (NIPS)*, 2017.

[48] Justin Gilmer, Samuel S. Schoenholz, Patrick F. Riley, Oriol Vinyals, and George E. Dahl. Neural message passing for quantum chemistry. *CoRR*, abs/1704.01212, 2017.

[49] Yunsheng Shi, Zhengjie Huang, Wenjin Wang, Hui Zhong, Shikun Feng, and Yu Sun. Masked label prediction: Unified massage passing model for semi-supervised classification. *CoRR*, abs/2009.03509, 2020.

[50] Vijay Prakash Dwivedi and Xavier Bresson. A generalization of transformer networks to graphs. *CoRR*, abs/2012.09699, 2020.

[51] Sanmit Narvekar, Bei Peng, Matteo Leonetti, Jivko Sinapov, Matthew E. Taylor, and Peter Stone. Curriculum learning for reinforcement learning domains: A framework and survey. *CoRR*, abs/2003.04960, 2020.

[52] Matthew E. Taylor and Peter Stone. Transfer learning for reinforcement learning domains: A survey. *Journal of Machine Learning Research*, 10(56):1633–1685, 2009.

[53] Alessandro Lazaric, Marcello Restelli, and Andrea Bonarini. Transfer of samples in batch reinforcement learning. pages 544–551, 01 2008.

[54] Matthew J. Hausknecht and Peter Stone. Deep recurrent q-learning for partially observable mdps. *CoRR*, abs/1507.06527, 2015.

[55] Sepp Hochreiter and Jürgen Schmidhuber. Long Short-Term Memory. *Neural Computation*, 9(8):1735–1780, 11 1997.

[56] KyungHyun Cho, Bart van Merrienboer, Dzmitry Bahdanau, and Yoshua Bengio. On the properties of neural machine translation: Encoder-decoder approaches. *CoRR*, abs/1409.1259, 2014.

[57] V.G. Rao and D.S. Bernstein. Naive control of the double integrator. *IEEE Control Systems Magazine*, 21(5):86–97, 2001.

[58] Zengyi Qin, Kaiqing Zhang, Yuxiao Chen, Jingkai Chen, and Chuchu Fan. Learning safe multi-agent control with decentralized neural barrier certificates. *CoRR*, abs/2101.05436, 2021.

[59] Albert Reuther, Jeremy Kepner, Chansup Byun, Siddharth Samsi, William Arcand, David Bestor, Bill Bergeron, Vijay Gadepally, Michael Houle, Matthew Hubbell, Michael Jones, Anna Klein, Lauren Milechin, Julia Mullen, Andrew Prout, Antonio Rosa, Charles Yee, and Peter Michaleas. Interactive supercomputing on 40,000 cores for machine learning and data analysis. In *2018 IEEE High Performance extreme Computing Conference (HPEC)*, pages 1–6. IEEE, 2018.

[60] Adam Paszke, Sam Gross, Francisco Massa, Adam Lerer, James Bradbury, Gregory Chanan, Trevor Killeen, Zeming Lin, Natalia Gimelshein, Luca Antiga, Alban Desmaison, Andreas Köpf, Edward Z. Yang, Zach DeVito, Martin Raison, Alykhan Tejani, Sasank Chilamkurthy, Benoit Steiner, Lu Fang, Junjie Bai, and Soumith Chintala. Pytorch: An imperative style, high-performance deep learning library. *CoRR*, abs/1912.01703, 2019.

[61] Matthias Fey and Jan E. Lenssen. Fast graph representation learning with PyTorch Geometric. In *ICLR Workshop on Representation Learning on Graphs and Manifolds*, 2019.

A Baseline Implementation Sources

We modified the codebases from the official implementations for the GPG, DGN, EMP, and MAPPO baselines. We also adapted the codebase for MADDPG, MATD3, VDN and QMIX for our experiments which was benchmarked on other standard environments. The links for all these implementations are listed below.

- GPG: https://github.com/arbaazkhan2/gpg_labeled
- DGN: https://github.com/jiechuanjiang/pytorch_DGN
- EMP: https://github.com/sumitsk/marl_transfer
- MAPPO: https://github.com/marlbenchmark/on-policy
- MADDPG, MATD3, QMIX, VDN: https://github.com/marlbenchmark/off-policy

B Hyperparameters

We performed a hyperparameter search for these algorithms by varying the learning-rates, network size and a few algorithm specific parameters. We observed that the hyperparameters used in the original implementation gave the best performance, and used those same values for our experiments as well.

Table 3 lists the hyperparameters specific to the InforMARL implementation. Here, "entity embedding layer dim" and "entity hidden dim" refer to the embedding layer input and output dimension respectively which is used to process the `entity-type` variable in the graph. "add self loop" refers to whether a self-loop should be added while constructing the agent-entity graph. "gnn layer hidden dim" is the output dimension of each layer in the graph transformer. "num gnn heads" and "num gnn layers" are the number of heads in the attention layer and number of attention layers used in the graph transformer. "gnn activation" is the activation function used after each layer in the GNN module.

Hyperparameters	Value
entity embedding layer dim	3
entity hidden dim	16
num embedding layer	1
add self loop	False
gnn layer hidden dim	16
num gnn heads	3
num gnn layers	2
gnn activation	ReLU

Table 3: Hyperparameters used in InforMARL

Tables 4, 5, 6 list the hyperparameters common for the InforMARL, MAPPO, MADDPG, MATD3, QMIX and VDN implementations. For MADDPG, MATD3, MAPPO, QMIX, VDN and InforMARL, "batch size" refers to the number of environment steps collected before updating the policy via gradient descent. "mini batch" refers to the number of mini-batches a batch of data is split into. "gain" refers to the weight initialization gain of the last network layer for the actor network. "num envs" refers to the number of parallel roll out threads used to collect state-transition tuples.

C Computational Environment

Our models were trained on a server with 40 Intel Xeon Gold 6248 @ 2.50 GHz processor cores and 2 NVIDIA Volta V100 graphics cards. Our code uses PyTorch [60] version 1.11.0, CUDA version 11.3, and PyTorch Geometric Library [61] version 2.0.4.

Common Hyperparameters	Value
recurrent data chunk length	10
gradient clip norm	10.0
gae lambda	0.95
gamma	0.99
value loss	huber loss
huber delta	10.0
batch size	num envs $\times$ buffer length $\times$ num agents
mini batch size	batch size / mini-batch
gain	0.01
network initialization	Orthogonal
optimizer	Adam
optimizer epsilon	1e-5
weight decay	0
use reward normalization	True
use feature normalization	True

Table 4: Common Hyperparameters used in MAPPO and InforMARL

Common Hyperparameters	Value
gradient clip norm	10.0
random episodes	5
epsilon	$1.0 \rightarrow 0.05$
epsilon anneal time	50000 timesteps
train interval	1 episode
gamma	0.99
critic loss	mse loss
buffer size	5000 episodes
batch size	32 episodes
optimizer	Adam
optimizer eps	1e-5
weight decay	0
network initialization	Orthogonal
use reward normalization	True
use feature normalization	True

Table 5: Common Hyperparameters used in MADDPG, MATD3, QMIX, VDN

D Full Comparison

We showcase the learning curves of all the baseline algorithms, including MADDPG, RMADDPG, MATD3, QMIX, VDN, GPG (static), and DGN in Figure 6.

Common Hyperparameters	Value
num envs	128
buffer length	25
num GRU layers	1
RNN hidden state dim	64
fc layer hidden dim	64
num fc	2
num fc after	1

Table 6: Common Hyperparameters used in MAPPO, MADDPG, MATD3, QMIX, VDN and InforMARL

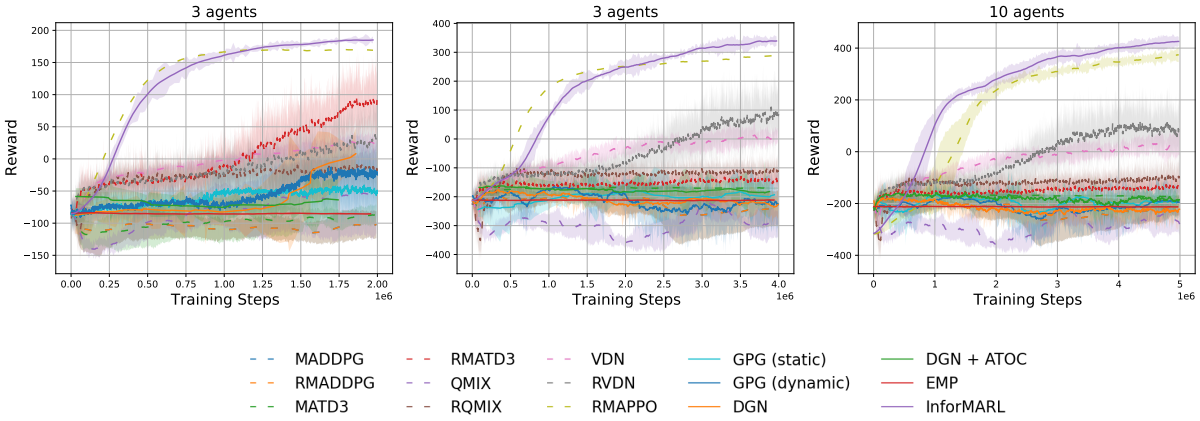

Figure 6: A thorough comparison of InforMARL with baselines. The algorithms that use global information modes are represented with dashed lines and the algorithms that use local information modes are represented with solid lines. The means and standard deviations of the rewards over training with five random seeds are shown.